Bioorganic & Medicinal Chemistry xxx (2014) xxx–xxx

Contents lists available at ScienceDirect

Bioorganic & Medicinal Chemistry

journal homepage: www.elsevier.com/locate/bmc

Structure-based efforts to optimize a non-β-lactam inhibitor of AmpC β-lactamase

Jenna M. Hendershot [a,†], Uma J. Mishra [b], Robert P. Smart [b], William Schroeder [b], Rachel A. Powers [a,b,*]

[a] Cell and Molecular Biology Program, Grand Valley State University, Allendale, MI 49401, United States
[b] Department of Chemistry, Grand Valley State University, Allendale, MI 49401, United States

ARTICLE INFO

Article history:
Received 14 February 2014
Revised 16 April 2014
Accepted 25 April 2014
Available online xxxx

Keywords:
Antibiotic resistance
Structure-based drug design
X-ray crystallography

ABSTRACT

β-Lactams are the most widely prescribed class of antibiotics, yet their efficacy is threatened by expression of β-lactamase enzymes, which hydrolyze the defining lactam ring of these antibiotics. To overcome resistance due to β-lactamases, inhibitors that do not resemble β-lactams are needed. A novel, non-β-lactam inhibitor for the class C β-lactamase AmpC (3-[(4-chloroanilino)sulfonyl]thiophene-2-carboxylic acid; K_i 26 μM) was previously identified. Based on this lead, a series of compounds with the potential to interact with residues at the edge of the active site were synthesized and tested for inhibition of AmpC. The length of the carbon chain spacer was extended by 1, 2, 3, and 4 carbons between the integral thiophene ring and the benzene ring (compounds **4**, **5**, **6**, and **7**). Compounds **4** and **6** showed minimal improvement over the lead compound (K_i 18 and 19 μM, respectively), and compound **5** inhibited to the same extent as the lead. The X-ray crystal structures of AmpC in complexes with compounds **4**, **5**, and **6** were determined. The complexes provide insight into the structural reasons for the observed inhibition, and inform future optimization efforts in this series.

1. Introduction

Antibiotic resistance has emerged as one of the leading public health crises of the 21st century.[1–3] A crucial part of this problem is the increasingly widespread resistance to β-lactam antibiotics, such as the penicillins and cephalosporins (Fig. 1), mainly due to their extensive use and misuse.[4] Several mechanisms can contribute to the resistant phenotype. However, the most prevalent is the expression of β-lactamase enzymes. These enzymes hydrolyze the four-membered lactam ring of the antibiotic (Fig. 1A), rendering it ineffective and unable to inhibit its intended target, the cell wall transpeptidase enzyme.

To overcome resistance due to β-lactamases, compounds that inhibit these enzymes were introduced and are generally co-administered with a partner β-lactam antibiotic.[5] Most are derived from natural sources and contain the same defining β-lactam ring as their antibiotic counterparts (Fig. 1B). Reliance on this same core structure allows bacteria to recognize the lactam ring and easily evolve resistance to these similar molecules. Inhibitors that do not resemble β-lactams would require bacteria to develop novel resistance mechanisms.

Previous research identified a non-covalent, non-β-lactam inhibitor for the class C β-lactamase AmpC (3-[(4-chloroanilino)sulfonyl]thiophene-2-carboxylic acid; K_i 26 μM) that was found to bind competitively and reversibly (Fig. 1C).[6] The X-ray crystal structure of AmpC in complex with this lead compound suggested numerous features of the inhibitor were essential for the binding affinity. Several analogs of this lead were tested in inhibition assays to better understand the SAR of this compound. Based on these previous studies, some features of this inhibitor were determined to contribute to recognition by key active site residues on the enzyme. The carboxylate group was shown to bind in the putative oxyanion hole,[7] making hydrogen bonds with main chain atoms of the catalytic serine (Ser64) and Ala318. The sulfonamide group and its orientation were important for binding and recognition by R1 side chain recognition residues (Asn152 and Ala318). Finally, the chlorophenyl ring was shown to stack with the conserved residue Tyr221.

Despite its modest inhibition, the 26 μM inhibitor was able to overcome resistance in bacterial cell culture, reducing the minimum inhibitory concentration (MIC) of the β-lactam ampicillin

Abbreviations: DMSO, dimethylsulfoxide; DMF, dimethylformamide; NMP, *N*-methylpyrrolidone; SAR, structure activity relationships.

* Corresponding author. Tel.: +1 616 331 2853; fax: +1 616 331 3230.
E-mail address: powersra@gvsu.edu (R.A. Powers).
† Current address: Biological Chemistry Department, University of Michigan, Ann Arbor, MI 48109, United States.

http://dx.doi.org/10.1016/j.bmc.2014.04.051
0968-0896/

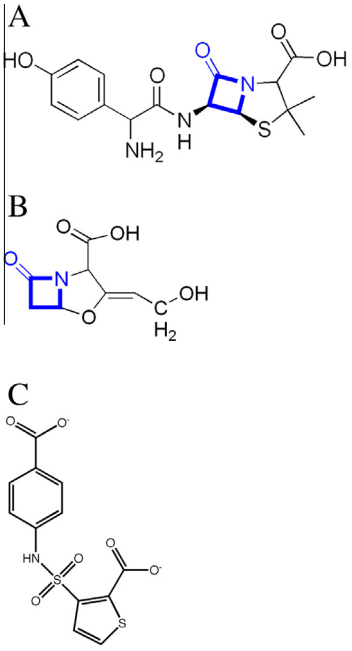

Figure 1. Structures of several ligands that bind to β-lactamase enzymes. (A) β-Lactam antibiotic (amoxicillin) with the four-membered ring highlighted. (B) Clavulanic acid, a β-lactamase inhibitor. (C) Lead compound (3-[(4-chloroanilino)sulfonyl]thiophene-2-carboxylic acid; K_i 26 μM).

four-fold in a resistant strain of *Escherichia coli* that overexpresses AmpC.[6] The novel chemical structure of this lead, along with its weak biological activity, made it a good candidate for optimization efforts to improve affinity and ultimately resulted in the identification of a 1.1 μM inhibitor (compound **1A**; Table 1) with improved activity against resistant bacteria.[8] This series of analogs explored the addition of different functional groups to the aryl ring. The best inhibitors (which include compound **1A**) share a carboxylate group addition to the aryl ring. The X-ray crystal structure of **1A** in complex with AmpC (PDB 1XGJ)[8] reveals that this carboxylate group points toward the solvent exposed entrance to the active site (Fig. 2).

Comparison of the structures of AmpC in complexes with both the 26 μM lead and compound **1A** reveals that a large portion of the active site remains open for possible interactions with an inhibitor, which could potentially improve the binding affinity. Asp123, Arg204, and Ser212 are located at the lip of the active site and are almost completely conserved in class C β-lactamases with observed substitutions maintaining the same charge or similar polarity. These polar residues could potentially allow for favorable interaction with inhibitors (Fig. 2). The carboxylate group addition to compound **1A** extended toward this area of the active site but made only a water-mediated hydrogen bond with Arg204 (Fig. 2). Increasing the size and flexibility of the compounds might allow for a direct ionic interaction between the carboxylate and Arg204 to be formed. It could also provide a more extensive sampling of this distal region of the active site, and possibly identify other residues at the edge of the active site for interaction with a more extended inhibitor.

Based on the previous set of analogs, the addition of a one-carbon linker between the sulfonamide and the phenyl ring provided an increase in flexibility and also preserved the same binding affinity as the lead.[8] In many of the previous analogs, the addition of a carboxylate to the aryl ring greatly improved the binding affinity, up to 30-fold in some cases.[8] We hypothesized that addition of a carboxylate to a more flexible compound might result in similar improvement in binding affinity. Additionally, a more flexible analog might be able to interact with distal residues in the open active site. We wondered what impact this would have on the binding affinity. A series of compounds based on the lead were synthesized where the length of the carbon chain between the sulfonamide group and the phenyl ring was extended by 1, 2, 3, and 4 carbons. The increased flexibility of the analogs would explore more of the active site and could probe for favorable interactions with active site lip residues to improve affinity.

The structure–activity relationship of this series was explored. Despite this design effort, the inhibitory activity of the compounds against AmpC did not drastically improve over the lead. Compound **5**, the compound that increased the chain length by two carbons

Table 1
Kinetic characterization of thiophene-carboxy derivatives against AmpC

Compound	Structure	K_i (μM)	Compound	Structure	K_i (μM)
Lead	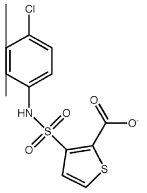	26[a]	**4**	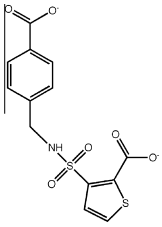	18
1	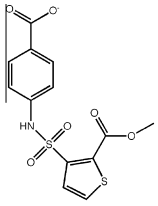	ND	**5**	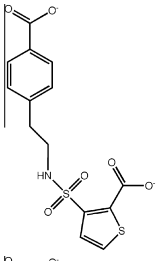	31 (26[c])
1A	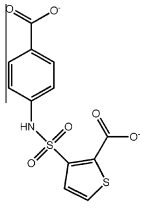	1.7 (1.1[b])	**6**	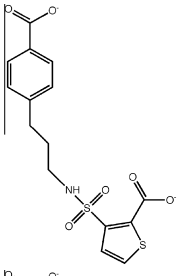	19
2	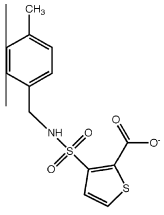	58	**7**	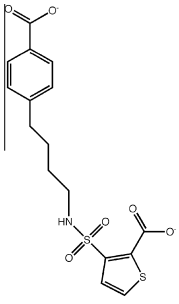	ND
3	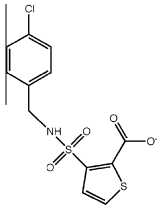	112			

[a] Powers (2002).[6]
[b] Reported in Tondi (2005).[8]
[c] Calculated by Lineweaver–Burk analysis.

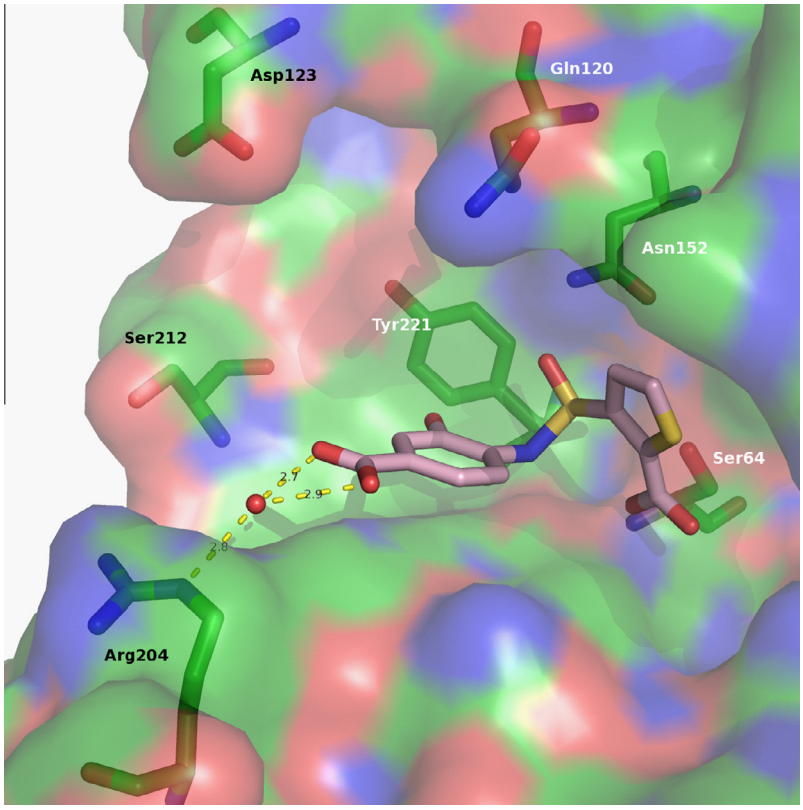

Figure 2. Surface representation of the AmpC/**1A** complex. Key active site residues important for recognition of the thiophene/sulfonamide core of the inhibitor (white labels). Lip residues (black labels) that were targeted for interaction with the extended, flexible series of analogs (Table 1). Carbon atoms for protein residues are colored green, carbons for the inhibitor are pink, nitrogens are blue, oxygens red and sulfurs yellow. All figures were created with PyMOL.[26]

had a K_i value of 26 μM, the same as the lead compound. Compounds **4** and **6**, the one and three carbon compounds, were slightly better than the lead, K_i values of 18 μM and 19 μM, respectively. To investigate the structural basis for inhibition, we co-crystallized each of the compounds **4**, **5**, and **6** with AmpC. The structures of each of these complexes provide information for future structure-based drug design against AmpC and underscore the difficulties in optimization of novel leads.

2. Results

2.1. Synthesis

The synthesis of methyl ester intermediates **1**–**4** was accomplished by reacting commercially available sulfonyl thiophene chloride with the free amine in anhydrous pyridine (Scheme 1). Each intermediate ester was characterized either through thin layer chromatography (TLC) or ^{1}H NMR. Each methyl ester was then hydrolyzed to the final carboxylic acid derivative using saponification conditions of sodium hydroxide and precipitation with HCl (Scheme 1; Table 1). Reactions were monitored using TLC, and final products were characterized by ^{1}H NMR, and ^{13}C NMR. The creation of compounds **5**, **6**, and **7** involved a multi-step synthesis of the free amine followed by coupling to sulfonyl chloride. The stepwise process to synthesize the free amine included Gabriel synthesis[9] followed by a Friedel Crafts acylation[10] and finally oxidation to the carboxylic acid by the haloform reaction (Scheme 2). Once the amine salt was synthesized, Schotten–Baumann[11] reaction conditions were used in order to couple the free amine to sulfonyl thiophene chloride.

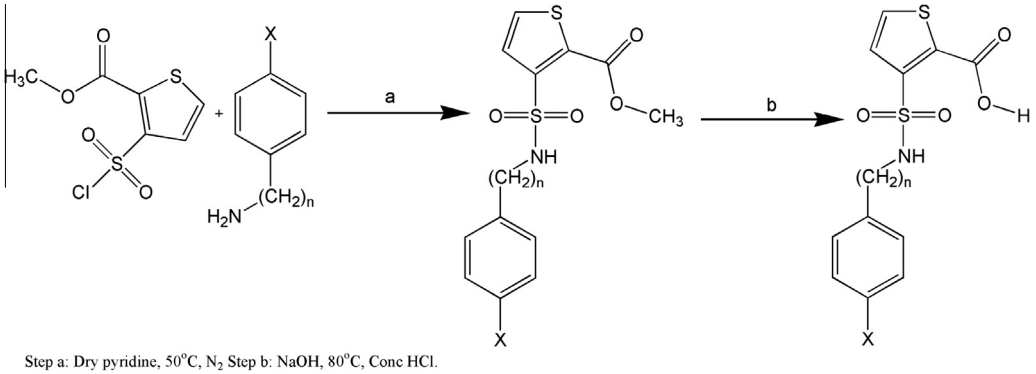

Scheme 1. Synthesis of 3-((4-chloroanilin)sulfonyl)thiophene-2-carboxylic acid derivatives compounds **1**–**4**. X = COOH (for **1**, **1A**), CH_3 (for **2**) or Cl (for **3**). n = 1 (for **4**).

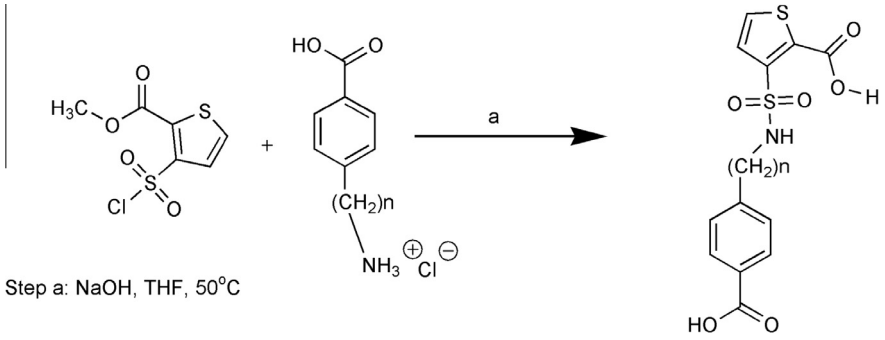

Scheme 2. Synthesis of 3-[(4-chloroanilin)sulfonyl]thiophene-2-carboxylic acid derivatives compounds **5**–**7**. $n = 2$, 3, or 4 for compounds **5**, **6**, and **7**, respectively.

2.2. Enzymology

Using an established enzyme assay,[6] each of the compounds was tested as an inhibitor of the class C β-lactamase AmpC (Table 1). The ester precursors were observed to be insoluble in assay buffer (50 mM Tris, pH 7.0) and were unable to be characterized kinetically. The seven free acids (**1A** and **2**–**7**) were evaluated, and IC_{50} and K_i values were determined (Table 1). Inhibition K_i values were obtained from IC_{50} plots assuming competitive inhibition.[12] The K_i value for compound **1A** was 1.7 μM, which is similar to the K_i determined by Tondi et al. (1.1 μM).[8]

Varying the substituent on the phenyl ring showed improved K_i values in the initial lead as compared to compound **1A**. Here, the replacement of the chlorine with a carboxylate group improved binding ~13-fold. With compounds **2**, **3**, and **4**, we further explored the impact of substitutions at this position. The methyl (**2**), chlorine (**3**) and carboxylate (**4**) substituents had K_i values of 58, 112 and 18 μM, respectively. Compounds **2** and **3** with the more nonpolar substituents bound with ~3-fold and 6-fold worse binding affinity as compared with compound **4** with the polar carboxylate substituent at the phenyl ring. Therefore, the remaining analogs contained a carboxylate substituent at this position and were further pursued to explore the effect of linker length.

With compound **4**, the linker length was increased by one carbon as compared with **1A**, and **4** was determined to have a K_i value of 18 μM. Increasing linker length by one carbon resulted in a ~10-fold reduction in K_i when compared to compound **1A** (K_i 1.1 μM). Compound **5** contained a two-carbon linker and was determined to have a K_i value of 31 μM, an approximate 2-fold reduction when compared to **4**. The K_i value for **5** was also obtained by varying both substrate and inhibitor concentrations, and this full kinetic analysis confirmed competitive inhibition (data not shown). Interestingly, the K_i value for compound **6**, which contained the three-carbon linker, was approximately the same as the one-carbon linker (**4**), with a K_i value of 19 μM. Overall the inhibitory activity of the compounds against AmpC was not drastically improved over the lead, but these results show that even with a one-carbon extension, addition of a carboxylate on the phenyl ring improves binding affinity (compound **4** vs compound **2**, **3**).

2.3. X-ray crystallographic structure determination

The X-ray crystal structures of AmpC in complexes with compounds **4**–**6** were determined to 1.9, 1.8, and 2.3 Å, respectively. The quality of the models was evaluated with MolProbity.[13] For the AmpC/**4** complex, 100% of the residues were in the allowed region of the Ramachandran plot, with 99.6% in the allowed region for AmpC/**5**, and 99.9% for AmpC/**6**. In all cases, AmpC crystallized in the space group C2 with a dimer in the asymmetric unit. Initial Fo-Fc difference density, contoured at 3.0 σ, indicated that the inhibitors were present in the active sites of the structures. The inhibitors were built into the structures using Coot[14] and refined with Refmac5[15] in the CCP4 Suite.[16] Overlays of each of these structures with the lead compound indicate a similar binding mode for the thiophene ring/sulfonamide core structure that is bound near the active site serine residue (Ser64). In every inhibitor conformation, the electron density for the core is very well defined. However, in the distal portion beyond the sulfonamide group, the electron density is much weaker, indicating the increased flexibility of this part of the inhibitor as it approaches solvent (Fig. 3). With increasing carbon spacer length, the distal portion of the inhibitor does indeed extend further out of the active site, away from the catalytic serine and toward residues Arg204, Asp123, and Ser212 that mark the edge of the active site.

In the AmpC/**4** complex, the position of the inhibitor in the active site was unambiguously identified in the B monomer only. The addition of a carboxylate to the benzene ring of compound **4** added four hydrogen bond interactions; three to water molecules (W78, W432, W433) and one to the main chain nitrogen of Ser212 (Fig. 4A). The interaction with Ser212 is a result of the increased length and flexibility afforded by the one-carbon extension to the linker. The slightly improved binding affinity (18 μM compared to 26 μM for the lead) may be attributed to the two additional hydrogen bonds made to the enzyme (Ser212 and Gln120). The favorable quadrupole stacking interaction with Tyr221 is also maintained in this complex.

In the AmpC/**5** complex, electron density for the inhibitor is observed in both monomers. The thiophene/sulfonamide core binds the same as the lead and 4, except the sulfonamide group of **5** does not make a hydrogen bond with Gln120. In the A monomer, a single conformation for **5** is present, with the trajectory of the carboxyphenyl ring extending toward the edge of the active site. The carboxylate group makes hydrogen bonds with Tyr221OH and the main chain oxygen of Ser212 (Fig. 4B). A similar conformation is also observed in the B monomer, but in addition to this, an alternate binding mode is adopted. The alternate conformation also extends out to solvent, and explores a different area of the active site. The carboxylate group now favorably interacts with Arg204 (hydrogen bond to Arg204N (2.8 Å) and ionic interactions, 3.5 Å). Due to the two-carbon linker, this inhibitor extends too far beyond Tyr221 to make the favorable quadrupole interactions observed in the lead and compound **4**, and the binding affinity (31 μM) was similar to the lead (26 μM).

With the longer linker of **6**, the carboxyphenyl ring is able to extend even further away from the center of the active site and toward the edge of the active site. However, the carboxylate functional group does not make any specific interactions with polar residues at the lip of the active site (e.g., Arg204, Asp123, or Ser212) in the B monomer, and in the A monomer, there is only a single hydrogen bond made between this group and a main chain

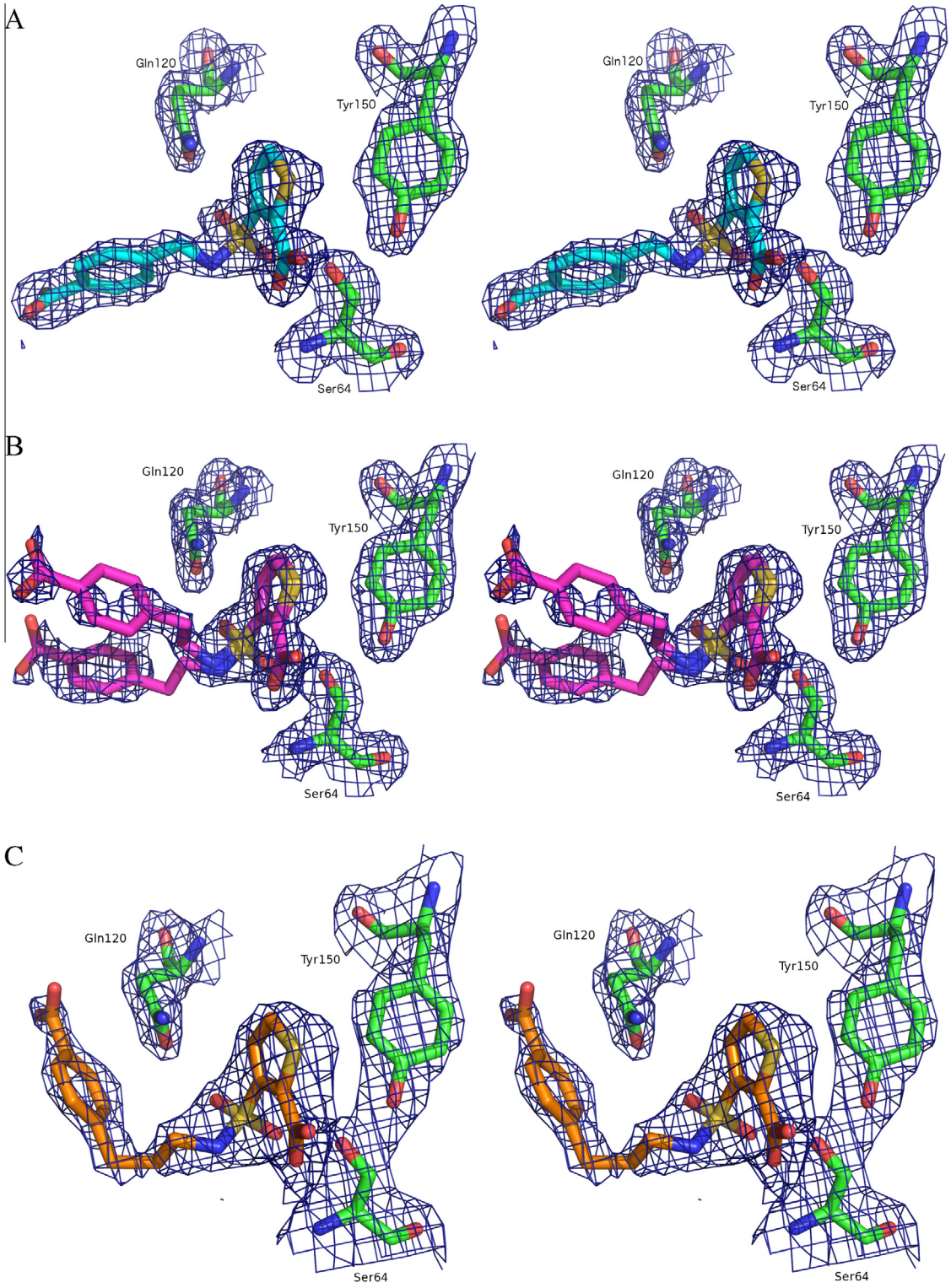

Figure 3. Stereo view $2F_o–F_c$ electron density maps contoured at 1 σ of the active site of AmpC in complexes with non-covalent inhibitors. (A) Compound **4**. (B) Compound **5**. (C) Compound **6**. Carbon atoms of the protein are colored green and of **4** are cyan, **5** are magenta and **6** are orange. Nitrogen atoms are blue, oxygen atoms red and sulfur atoms yellow. All figures were created with PyMOL.[26]

oxygen of His210 (Fig. 4C). The binding affinity was not significantly improved (K_i 19 μM), and the even longer three-carbon linker does not allow for quadrupole interactions with Tyr221. In the complex of AmpC with **6**, some evidence exists for a second conformation in the A monomer, but the density is so poorly defined that modeling it was not feasible. Compound **6** does bind differently in monomer A when compared to monomer B.

3. Discussion

β-Lactamases are the most widespread resistance mechanisms to β-lactam antibiotics, and there is a pressing need for novel, non-β-lactam drugs. A previously identified thiophene-based lead (3-[(4-chloroanilino)sulfonyl] thiophene-2-carboxylic acid; K_i 26 μM) was found to bind competitively and reversibly to AmpC,[6]

and its affinity was improved to 1.1 μM (compound **1A**) by replacing the chlorine of the lead with a carboxylate on the aryl ring.[8] The improvement was tentatively attributed to a water-mediated interaction between this carboxylate and Arg204 (1XGJ) at the entrance of the active site, although other possibilities could not be ruled out. We hypothesized that extension of the linker between the core structure of the lead and the aryl ring, coupled with the addition of the distal carboxylate, might result in a direct interaction with Arg204 and thereby improve binding affinity. Additionally, we wondered if increased flexibility in this series of analogs might identify other potential binding partners for the distal carboxylate at the edge of the active site.

The kinetic characterization coupled with representative crystal structures suggests that increasing the linker length in this series of analogs is not a rational approach to improving the affinity of this series. Other groups[17,18] have explored the inclusion of linkers, both rigid and flexible, as a way to improve binding affinity with varying degrees of success. In each instance, optimization of the length of the linker was essential. In our case, the addition of a one carbon linker to the lead resulted in compound **3**, which bound ~4.5-fold worse than the lead. Replacing the chlorine in **3** with a carboxylate resulted in a 6-fold reduction in the K_i value from 112 μM (**3**) to 18 μM (**4**). This trend was also observed when the chlorine of the lead was substituted for a carboxylate to produce compound **1A**.[8] Increasing linker length by another one or two carbons (compounds **5** and **6**, respectively) gives mixed results: the affinity of compound **5** is about two-fold worse than compound **4**, and the affinity of compound **6** returns to that of compound **4**. So while the affinity of this series of inhibitors can be improved by addition of a distal carboxylate, none inhibit as well as **1A**. To more fully explore why the design of this series was unsuccessful, the structures of three of these analogs were determined in complexes with AmpC.

Unfortunately, the structural basis for inhibition in this series is not easily explained by these complexes, although there are a few indications that might inform future design efforts. The structure of the lead molecule in complex with AmpC highlighted the importance of the thiophene/sulfonamide core and its hydrogen bonding interactions with Ser64 and Asn152, and quadrupole stacking with Tyr221.[6] In each of the complexes determined here, the interactions with Ser64 and Asn152 were maintained, and the electron density for the thiophene/sulfonamide core was much better defined than the portion beyond the sulfonamide group.

The quadrupole interactions between the aryl ring of the inhibitors and Tyr221 are not maintained in all of the complexes determined. These interactions are only observed in the complex with **4**, the one carbon extension. Increasing the carbon linker length any further, as with compounds **5** and **6**, results in the loss of the quadrupole interaction with Tyr221. Attractive nonbonded interactions between aromatic rings are prevalent in protein-ligand complexes; the energetic contributions for this type of interaction in protein/ligand complexes is suggested to be on the order of 1–2 kcal/mol.[19] This type of interaction has been determined to contribute to the binding affinity of other β-lactamase inhibitors, such as the arylboronic acids,[20–23] in addition to the lead compound in this series, and it appears to be advantageous to maintain this interaction in any future analogs.

As for unique interactions between the analogs and the enzyme, compounds **4**, **5**, and **6** make relatively few new interactions with AmpC, compared to the lead. In the AmpC/**4** complex, additional hydrogen bonds were formed between the core sulfonamide group and Gln120, and also the distal carboxylate and Ser212, thus providing one possible explanation for improved affinity. However, the residue that was targeted for direct interaction with the distal carboxylate, Arg204, does not interact with the carboxylate due to altered trajectory of **4** as compared to the lead. Compound **5** with a two carbon linker allows for hydrogen bonds to be formed with side chain atoms of both Arg204 and Ser212, located at the edge of the active site, but only in one of the two conformations observed. Despite the additional hydrogen bonds, this compound has a worse K_i value than **4**, which could be attributed to the loss of the quadrupole interactions with Tyr221. Compound **6**, with the three-carbon linker fails to make quadrupole interactions with Tyr221 or with any of the polar residues at the edge of the active site, and only a single hydrogen bond is made with a main chain carbonyl oxygen. Strangely, this lack of protein interactions with **6** translates into a K_i value similar to that of compound **4** that does make additional interactions with the enzyme.

The addition of a 1–4 carbon linker introduced length and flexibility within the series. We initially hypothesized that this flexibility would allow compounds to explore other possible binding partners present at the active site entrance, for example Asp123 and Ser212 (Figs. 2 and 5). All three of these residues are almost completely conserved in class C β-lactamases with observed substitutions maintaining the same charge or similar polarity (e.g., Arg204 → Lys; Asp123 → Glu; Ser212 → Thr/Asn). The increased flexibility of these molecules is evident in the crystal structures (Fig. 4). Multiple conformations are observed for the substituted aryl ring of compounds **5** and **6**, but not compound **4**. The longer linkers did allow these molecules to extend to the far edge of the active site and interact with Arg204 and Ser212 (Fig. 5). However, the affinity of these compounds derives from a balance between the favorable interactions formed with these polar residues and the entropic penalty for binding more flexible compounds. Overall, if these lip residues are to be exploited as binding sites in inhibitor design, a more rigid linker scaffold may be desired.

A longer linker in the presence of the distal carboxylate posed a trade-off between flexibility and solubility in our optimization attempts. Our data indicate that the three-carbon linker was the maximum length that was soluble in buffer. Within this series of new analogs, the one carbon linker was the optimal length for inhibition (compound **4**). This is a compromise that allowed additional hydrogen bonds with Gln120, but not so flexible that many binding modes are allowed. Overall, it appears that molecules with increased length do not behave as predicted.

In summary, our optimization efforts highlight the design challenges faced in attempting to improve a novel lead compound in a large, relatively open binding site. Increased flexibility due to entropic destabilization coupled with the loss of quadrupole interactions with Tyr221 appear to be detrimental to binding affinity in this series of analogs. Additionally, interactions with lip active site residues (such as Arg204, Ser212, and Asp123) are not significant, and do not translate to improved binding affinity as initially proposed. Future optimization efforts in this series of novel, non-covalent β-lactamase inhibitors should maintain edge-to-face aromatic interactions with Tyr221. Exploring the impact of adopting a more hindered, rigid linker system might also improve affinity by placing the trajectory of the inhibitor in a single conformation to favorably interact with residues in the AmpC active site.

4. Materials and methods

4.1. General information

All reagents were purchased from Sigma–Aldrich and used as received. Reactions were performed with dry glassware under an atmosphere of nitrogen or argon unless otherwise noted. ^{1}H and ^{13}C NMR spectra were measured on a JEOL JNM-ECP 300 FT-NMR (300 MHz) spectrometer using DMSO-d6 as a solvent. The values of the chemical shifts (δ) are given in ppm and coupling constants (J) in hertz. Peak multiplicities were given as follows: s, singlet; d,

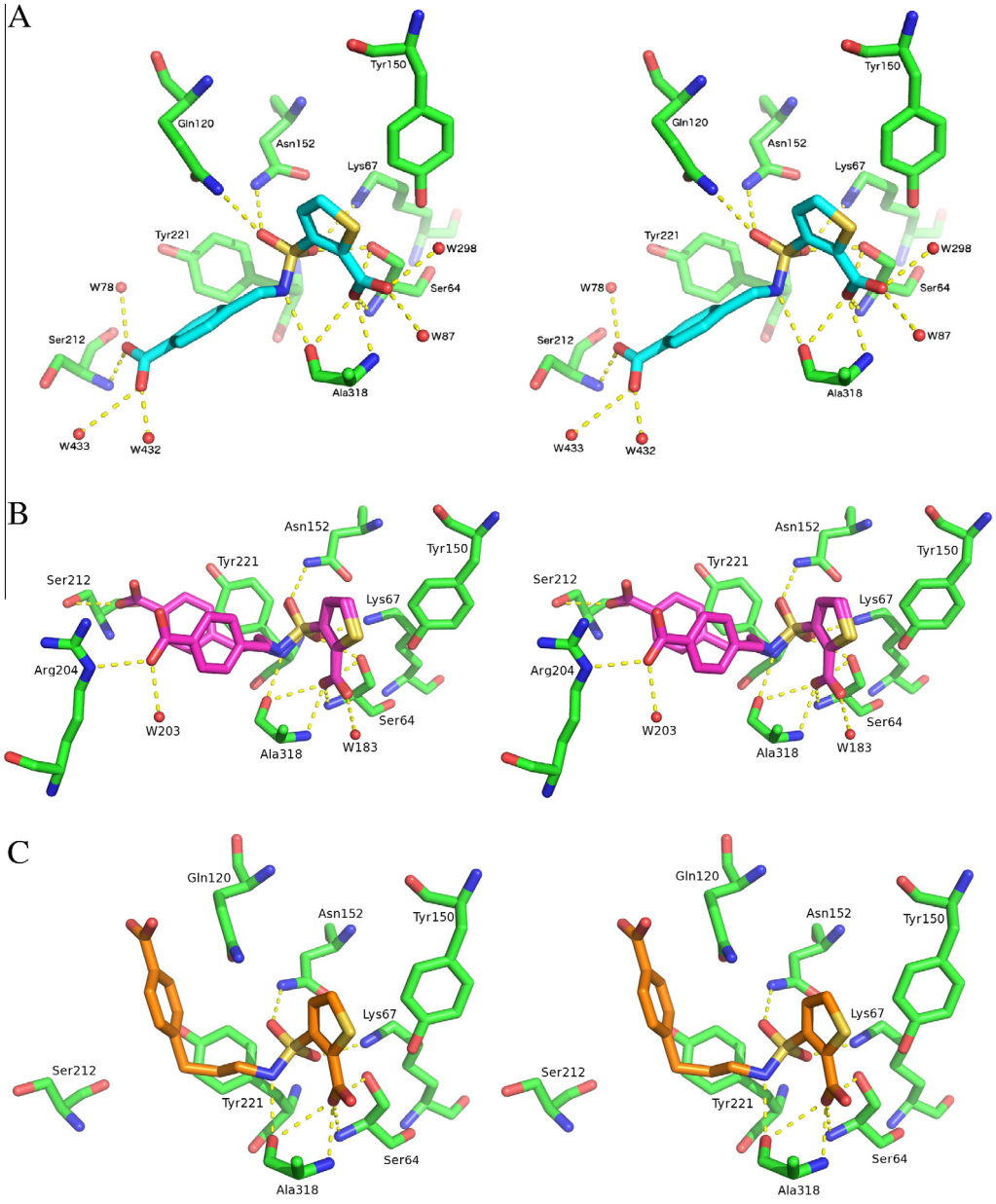

Figure 4. Hydrogen bonding interactions between AmpC and non-covalent inhibitors. (A) Compound **4**. (B) Compound **5**. (C) Compound **6**.

doublet; t, triplet; q, quartet; m, multiplet; and br, broad. Infrared spectra were recorded on a JASCO FTIR 4100. Mass spectrometry was performed on a single quadrupole MSQ mass spectrometer (Thermo Scientific) connected to the HPLC system (C18 column: HPLC water, acetonitrile and acetonitrile/formic acid). Elemental Analyses were performed by Atlantic Microlab, Inc, in Norcross, GA.

4.2. Synthesis

The mono methyl ester intermediates were synthesized by acylation of the amino acids with 2-carboxy-3-chlorosulfonyl thiophene. 4-Aminomethylbenzoic acid and 4-aminoethyl benzoic acid were purchased from Sigma–Aldrich. 4-Aminopropylbenzoic acid and 4-aminobutylbenzoic acid were prepared by published procedures. Saponification of the methyl esters afforded the diacids which were characterized by melting point, IR, ^{1}H NMR, ^{13}C NMR, ESI-MS, and elemental analysis.

4.2.1. 3-(4-Carboxybenzylsulfamoyl)thiophene-2-carboxylic acid (Compound 4)

Step 1-To a solution of 4-aminomethylbenzoic acid (0.7 g) and sodium carbonate (1.0 g) in water (25 mL) was added 2-carbomethoxy-3-chlorosulfoxylthiophene (1.2 g) in 1,2-dimethoxyethane (25 mL). The reaction mixture was stirred at room temperature for 30 min followed by an additional 30 min of stirring at 55 °C. Water (100 mL) was added and the resulting solution was filtered. The filtrate was acidified with concentrated HCl to give a precipitate of the methylester-acid. The crystals were collected by vacuum filtration, rinsed with water, and dried at 95 °C.

Step 2-A mixture of 3-(4-carboxybenzylsulfamoyl)thiophene-2-carboxylic acid methyl ester (0.7 g), potassium hydroxide (1.0 g), and water (10 mL) was heated at 85 °C for 40 min. After cooling to room temperature an additional 5 mL of water was added. The product was precipitated by the drop wise addition of concentrated hydrochloric acid. After drying at 95 °C, 3-(4-carboxybenzylsulfamoyl)thiophene-2-carboxylic acid was obtained in

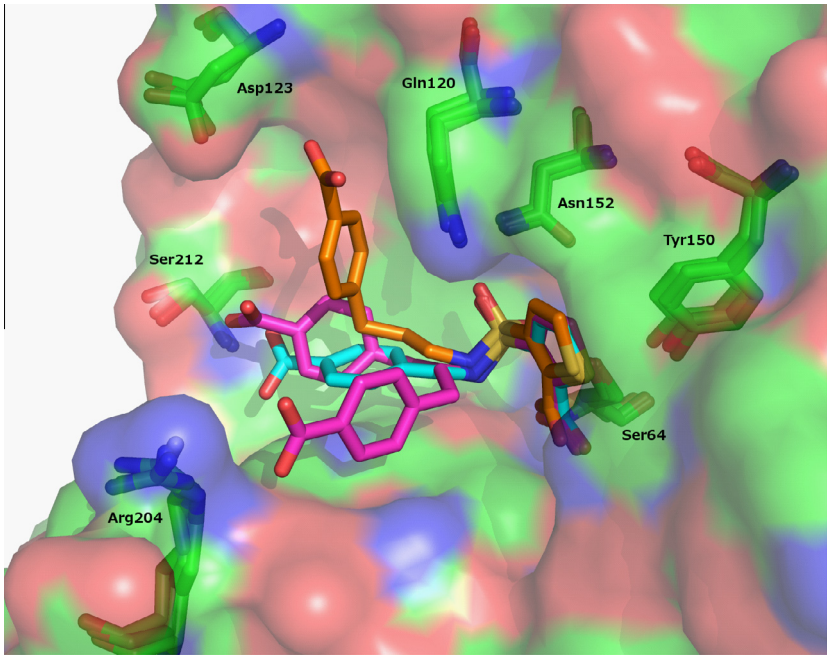

Figure 5. Overlay of the AmpC complexes with compounds **4**, **5**, and **6**. Carbon atoms of the protein are colored green and of **4** are cyan, **5** are magenta and **6** are orange. Nitrogen atoms are blue, oxygen atoms red and sulfur atoms yellow.

37% yield. Mp 184–187 °C. ^{1}H NMR: 7.9(d, *J = 5.2 Hz*, 1H); 7.8(d, *J = 8.4 Hz*, 2H); 7.4(d, *J = 5.2 Hz*, 1H); 7.3(d, *J = 8.4 Hz*, 2H), and 4.3(d, *J = 6.6 Hz*, 2H). ^{13}C NMR: 169, 163, 147, 134, 134, 134, 130, 128, 127, and 46. ESI-MS: 342 (M+1, positive mode). Anal. Calcd for $C_{13}H_{11}NO_6S_2$: C, 45.74; H, 3.25; N, 4.10. Found: C 45.47; H 3.24; N 4.18.

4.2.2. 3-(4-Carboxyphenylethylsulfamoyl)thiophene-2-carboxylic acid (Compound 5)

3-(4-Carboxyphenylethylsulfamoyl)thiophene-2-carboxylic acid methyl ester underwent saponification with potassium hydroxide and water. The product was precipitated by the drop wise addition of concentrated hydrochloric acid. After drying, 3-(4-carboxyphenylethyl-sulfamoyl)thiophene-2-carboxylic acid was obtained in 55% yield. Mp 209–210 °C. ^{1}H NMR: 7.9(d, *J = 5.2 Hz*, 1H); 7.8(d, *J = 8.4 Hz*, 1H); 7.4(d, *J = 5.2 Hz*, 1H); 7.2(d, *J = 8.4 Hz*, 1H), 3.2(m, 2H), and 2.8(m, 2H). ^{13}C NMR: 169, 163, 145,134, 134, 134, 130, 128, 128, 127, 43, and 34. ESI-MS: 356 (M+1, positive mode). Anal. Calcd for $C_{14}H_{13}NO_6S_2$: C 47.31; H 3.69; N 3.94. Found: C 47.44; H 3.78; N 3.95.

4.2.3. 3-(4-Carboxyphenylpropylsulfamoyl)thiophene-2-carboxylic acid (Compound 6)

3-(4-Carboxyphenylpropylsulfamoyl)thiophene-2-carboxylic acid methyl ester underwent saponification as described above in 63% yield. Mp 190–193 °C. ^{1}H NMR: 7.8(d, *J = 5.2 Hz*, 1H); 7.8(d, *J = 8.3 Hz*, 2H); 7.4(d, *J = 5.2 Hz*, 1H); 7.2(d, *J = 8.3 Hz*, 2H), 2.9(t, *J = 7.7 Hz*, 2H), 2.6(t, *J = 7.7 Hz*, 2H), and 1.7(m, 2H). ^{13}C NMR: 169, 163, 147, 134, 134, 134, 130, 128, 128, 127, 42, 30, and 28. ESI-MS: 370 (M+1, positive mode). Anal. Calcd for $C_{15}H_{15}NO_6S_2$: C 48.77; H 4.09; N 3.79. Found: C 48.66; H 4.06; N 3.84.

4.2.4. 3-(4-Carboxyphenylbutylsulfamoyl)thiophene-2-carboxylic acid (Compound 7)

55% yield. Mp 155–157 °C. ^{1}H NMR: 7.9(d, *J = 5.2 Hz*, 1H); 7.8(d, *J = 8.4 Hz*, 1H); 7.4(d, *J = 5.2 Hz*, 1H); 7.3(d, *J = 8.4 Hz*, 1H), 2.9 (m, 2H), 2.5(m, 2H), 1.4(m, 2H), and 1.31(m, 2H). ^{13}C NMR: 169, 163, 148, 134, 134, 134, 130, 128, 128, 127, 43, 35, 29, and 28. ESI-MS: 384 (M+1, positive mode). Anal. Calcd for $C_{16}H_{17}NO_6S_2$: C 50.12; H 4.47; N 3.65. Found: C 50.39; H 4.45; N 3.72.

4.3. Enzymology

AmpC was expressed and purified as previously described.[7] Kinetic measurements were performed using nitrocefin as substrate in 50 mM Tris, pH 7.0, and monitored on an Agilent HP 8453 UV–vis spectrophotometer at 482 nm. The K_m of nitrocefin for AmpC in this buffer was determined to be 127 μM. The concentration of enzyme in all reactions was 1.25 nM. IC_{50} values were determined at a substrate concentration of 200 μM. K_i values were obtained by comparison of progress curves in the presence and absence of inhibitor and assumed competitive inhibition.[12,24] Sufficient inhibitor was used to give at least 50% inhibition. Inhibitors were dissolved in DMSO at a concentration of 50 mM; dilute stock solutions were subsequently prepared as necessary, so that the concentration of DMSO in assays was 5% or less. Dilution of compound **7** from the stock solution into assay buffer resulted in precipitation of **7**. Preparation of stock solutions of **7** in dimethylformamide (DMF), or *N*-methylpyrrolidone (NMP) was also attempted, but **7** still precipitated when added to assay buffer. Therefore, the inhibition of AmpC by this compound was not measured. For compound **5**, the K_i value was also determined by Lineweaver-Burk analysis of multiple substrate (50, 100, 200, and 285 μM) and inhibitor (0, 20, 30, 50 μM) concentrations. Linear regression was performed in Microsoft Excel. The value obtained in this manner is consistent with that obtained by using the IC_{50} value.

4.4. Crystal growth and structure determination

Co-crystals of AmpC with each of the inhibitors were grown by vapor diffusion in hanging drops over 1.7 M potassium phosphate, pH 8.7, at room temperature using microseeding. Crystals appeared between 3–5 days after equilibration at room temperature. The concentration of AmpC was 3–4 mg/mL, and the concentration of the inhibitors was 1 mM. Crystals were harvested with a

Table 2
Crystallographic statistics for complexes of AmpC with compounds **4**, **5**, and **6**

	AmpC/**4**	AmpC/**5**	AmpC/**6**
Cell constants (Å, °)	a = 118.4, b = 76.7, c = 97.6; β = 115.6	a = 118.6, b = 77.2, c = 97.6; β = 115.4	a = 118.9, b = 77.7, c = 98.4; β = 115.4
Space group	C2	C2	C2
Resolution (Å)	50–1.90 (1.97–1.90)[a]	50–1.76 (1.82–1.76)	50–2.3 (2.38–2.30)
Unique reflections	62,237	70,212	34,262
Total observations	230,181	239,983	127,338
R_{merge} (%)	9.2 (36.8)	4.6 (21.3)	6.7 (36.6)
Completeness (%)	99.9 (100)	88.7 (86.4)	94.7 (99.2)
$\langle I/\sigma_I \rangle$	10.2	23.2	16.6
R_{cryst}, R_{free} (%)	16.9, 21.2	20.5 (24.4)	18.1, 25.5
Average B factors			
Protein atoms (Å^2)	24.3	31.6	46.8
Inhibitor atoms (Å^2)	39.8[b]	53.7[c]	62.8[d]
Waters (Å^2)	34.3	37.1	47.1

[a] Values in parentheses are for the highest resolution shell.
[b] Calculated for all 22 atoms of inhibitor present in B monomer only.
[c] Calculated for 69 inhibitor atoms, which is bound in a single conformation in the A monomer and in two conformations in the B monomer.
[d] Calculated for 48 atoms of the inhibitor.

nylon loop and immersed in a cryoprotectant solution containing 1.7 M potassium phosphate, pH 8.7, 20% sucrose for approximately 30 s and then flash cooled in liquid nitrogen. Data were measured from single crystals on the LS-CAT and DND-CAT beam lines (21-ID-D and 5-ID-B) of the Advanced Photon Source at Argonne National Lab at 100 K using a Mar CCD detector.

Reflections were indexed, integrated, and scaled using HKL2000[25] (Table 2). The space group was C2, with two AmpC molecules in the asymmetric unit. The structures of the complexes were determined using a native apo AmpC structure (PDB entry 1KE4, with water molecules and ions removed), as the initial phasing model. The structure was refined using REFMAC5[15] in the CCP4 program suite.[16] Electron density maps were calculated with REFMAC and used to build the protein model in the program Coot.[14] The inhibitors were each built into the initial observed difference density in each active site of the asymmetric unit, and the structures of the complexes were further refined using REFMAC (Table 2). In the final model, each molecule contained 358 residues, with one exception in the A monomer of AmpC/**4**, which only contained 352 residues. The structures have been deposited with the PDB as 4JXS for AmpC/**4**, 4JXV for AmpC/**5**, and 4JXW for AmpC/**6**.

Acknowledgments

The authors would like to thank LS-CAT and DND-CAT at the Advanced Photon Source (APS) for the use of synchrotron radiation. Use of the APS was supported by the U.S. Department of Energy, Office of Science, Office of Basic Energy Sciences, under Contract No. DE-AC02-06CH11357. Use of the LS-CAT Sector 21 was supported by the Michigan Economic Development Corporation and the Michigan Technology Tri-Corridor for the support of this research program (Grant 085P1000817). We thank the NSF-Advance program for a professional development grant (to RAP). We thank Jim O'Keefe at the Annis Water Resources Institute for performing the mass spectrometry analyses.

References and notes

1. Fisher, J. F.; Meroueh, S. O.; Mobashery, S. *Chem. Rev.* **2005**, *105*, 395.
2. Neu, H. C. *Science* **1992**, *1064*, 257.
3. Davies, J.; Davies, D. *Microbiol. Mol. Biol. Rev.* **2010**, *74*, 417.
4. Bush, K. *Ciba Found. Symp.* **1997**, *207*, 152.
5. Sutherland, R. *Trends Pharmacol. Sci.* **1991**, *12*, 227.
6. Powers, R. A.; Morandi, F.; Shoichet, B. K. *Structure* **2002**, *1013*, 10.
7. Usher, K. C.; Blaszczak, L. C.; Weston, G. S.; Shoichet, B. K.; Remington, S. J. *Biochemistry* **1998**, *37*, 16082.
8. Tondi, D.; Morandi, F.; Bonnet, R.; Costi, M. P.; Shoichet, B. K. *J. Am. Chem. Soc.* **2005**, *127*, 4632.
9. Gibson, M. S. ; Bradshaw, R. W. *Angew. Chem., Int. Ed. Engl.* **1968**, *7*, 919.
10. Heaney, H. *Compr. Org. Synth.* **1991**, *2*, 733.
11. Sonntag, N. O. V. *Chem. Rev.* **1953**, *52*, 237.
12. Waley, S. G. *Biochem. J.* **1982**, *205*, 631.
13. Chen, V. B.; Arendall, W. B., 3rd; Headd, J. J.; Keedy, D. A.; Immormino, R. M.; Kapral, G. J.; Murray, L. W.; Richardson, J. S.; Richardson, D. C. *Acta Crystallogr. D Biol. Crystallogr.* **2010**, *66*, 12.
14. Emsley, P.; Cowtan, K. *Acta Crystallogr. D Biol. Crystallogr.* **2004**, *60*, 2126.
15. Murshudov, G. N.; Vagin, A. A.; Dodson, E. J. *Acta Crystallogr. D Biol. Crystallogr.* **1997**, *53*, 240.
16. Collaborative Computational Project, Number 4 *Acta Crystallogr. D Biol. Crystallogr.* **1994**, *50*, 760.
17. Bodill, T.; Conibear, A. C.; Mutorwa, M. K.; Goble, J. L.; Blatch, G. L.; Lobb, K. A.; Klein, R.; Kaye, P. T. *Bioorg. Med. Chem.* **2013**, *21*, 4332.
18. LaFrate, A. L.; Carlson, K. E.; Katzenellenbogen, J. A. *Bioorg. Med. Chem.* **2009**, *17*, 3528.
19. Burley, S. K.; Petsko, G. A. *Science* **1985**, *229*, 23.
20. Powers, R. A.; Blazquez, J.; Weston, G. S.; Morosini, M. I.; Baquero, F.; Shoichet, B. K. *Protein Sci.* **1999**, *8*, 2330.
21. Powers, R. A.; Shoichet, B. K. *J. Med. Chem.* **2002**, *45*, 3222.
22. Tondi, D.; Powers, R. A.; Caselli, E.; Negri, M. C.; Blazquez, J.; Costi, M. P.; Shoichet, B. K. *Chem. Biol.* **2001**, *8*, 593.
23. Weston, G. S.; Blazquez, J.; Baquero, F.; Shoichet, B. K. *J. Med. Chem.* **1998**, *41*, 4577.
24. Chou, T. C. *Mol. Pharmacol.* **1974**, *10*, 235.
25. Otwinowski, Z.; Minor, W. *Methods Enzymol.* **1997**, *276*, 307.
26. DeLano, W. L.; Schrodinger LLC, **2010**.